The University of Tehran Press

Pollution

Print ISSN: 2383-451X
Online ISSN: 2383-4501

https://jpoll.ut.ac.ir/

Enhancing Microplastic Removal Efficiency Through Fe-based Coagulation: Insights from Response Surface Methodology and Machine Learning

Aan Priyanto[1] | Dian Ahmad Hapidin[1]✉ | Dhewa Edikresnha[1] | Khairurrijal Khairurrijal[1,2]✉

1. Research Group of Physics and Technology of Advanced Materials, Department of Physics, Faculty of Mathematics and Natural Sciences, Institut Teknologi Bandung, Jalan Ganesa No. 10, Bandung Jawa Barat 40132, Indonesia
2. Department of Physics, Faculty of Science, Institut Teknologi Sumatera, Jalan Terusan Ryacudu, Lampung Selatan, Lampung 35365, Indonesia

Article Info

Article type:
Research Article

Article history:
Received: 16 November 2025
Revised: 10 April 2026
Accepted: 15 April 2026

Keywords:
Microplastics; Coagulation; Iron-Based Coagulant; Response Surface Methodology; Machine Learning; Removal Efficiency

ABSTRACT

Microplastic pollution poses a major global environmental threat, demanding effective removal strategies. Coagulation is among the most practical methods due to its cost efficiency, simplicity, and high performance, with iron-based (Fe-based) coagulants showing particular environmental and operational advantages. However, integrated approaches combining statistical and machine learning optimization for different microplastic types and sizes remain limited. This study applied a hybrid Response Surface Methodology (RSM) and machine learning framework to optimize Fe-based coagulation for polyethylene terephthalate (PET), polyethylene (PE), and polypropylene (PP) microplastics of various sizes. A Box–Behnken design (15 runs per polymer) was used, totaling 135 experiments. Removal efficiency was quantified gravimetrically after floc separation and drying. The optimized process achieved a maximum removal efficiency of (94.9 ± 0.2)%, comparable to many previous reports. RSM yielded the lowest mean prediction error (1.80%), surpassing Linear Regression (2.74%) and Artificial Neural Network (5.02%) models trained using k-fold cross-validation to mitigate overfitting. Coagulant dose was identified as the most influential variable, followed by polyacrylamide (PAM) dose and pH. These findings provide a robust, data-driven framework for optimizing microplastic coagulation and highlight key operational factors governing efficient removal.

Cite this article: Priyanto, A., Ahmad Hapidin, D., Edikresnha, D., & Khairurrijal, Kh. (2026). Enhancing Microplastic Removal Efficiency Through Fe-based Coagulation: Insights from Response Surface Methodology and Machine Learning. *Pollution*, 12(2), 533-544.
https://doi.org/10.22059/poll.2026.406372.3196

DOI: https://doi.org/10.22059/poll.2026.406372.3196

INTRODUCTION

Microplastic pollution in aquatic environments has become a major global concern. Numerous studies have confirmed their widespread presence in freshwater, coastal, and marine ecosystems (Rossatto et al., 2023), as well as in aquatic organisms such as fish, shrimp, clams, and mussels (Tursi et al., 2022). Microplastics have also been detected in terrestrial animals, including chickens (Huo et al., 2025), sheep, and cattle (Bahrani et al., 2024), likely originating from contaminated water or feed. Evidence further shows their uptake by agricultural crops, including vegetables (Liu et al., 2025), fruits (Mandal, 2024), and rice (Bhavsar et al., 2024), providing additional pathways into the food chain. Consequently, microplastics have been

*Corresponding Author Email: *dian.ahmad@itb.ac.id*
krijal@itb.ac.id

detected in human tissues and prolonged exposure is suspected to contribute to hormonal disruption, inflammation, reproductive disorders, and cancer (Chartres et al., 2024). Hence, developing effective methods to remove microplastics from water is vital for protecting human health and water quality.

Various removal techniques have been explored, including coagulation (Thathsarani et al., 2025), filtration (Garfansa et al., 2024), ozonation (Ziembowicz & Kida, 2024) and phytoremediation (Yin et al., 2025). Among these, coagulation stands out for its cost-effectiveness, simplicity, and high efficiency (Oh et al., 2023). It operates primarily through charge neutralization and sweep flocculation, aggregating destabilized particles into larger flocs removable from water (Bratby, 2016). Coagulant ions, introduced chemically or electrochemically (Shen et al., 2022), promote aggregation via electrostatic and surface interactions (Tang et al., 2022). Metal-based coagulants of Fe, Al, and Mg have achieved microplastic removal efficiencies between 10% and >90%, especially when combined with coagulant aids such as polyacrylamide (PAM) (Chen et al., 2020, 2021). Among these, Fe-based coagulants are favored for their low toxicity, minimal residual metals, and superior floc settling (Tan et al., 2024), making them suitable for microplastic removal in sustainable water treatment.

Despite their wide application, critical gaps remain. Most studies focus on polyethylene (PE), neglecting other polymers prevalent in real environments (Wang et al., 2021), such as polypropylene (PP) and polyethylene terephthalate (PET). Furthermore, while parameters like pH, coagulant dosage, and coagulant aid concentration are known to affect performance, their relative significance has rarely been systematically evaluated or compared across optimization strategies. Notably, comparisons between classical methods like Response Surface Methodology (RSM) and machine learning approaches on small designed datasets remain scarce, and the interpretability of machine learning models is still limited without tools such as SHAP (SHapley Additive exPlanations).

This study addresses these gaps by integrating RSM and machine learning for Fe-based coagulation of PE, PP, and PET microplastics. RSM enables parametric analysis with minimal experimental runs (Priyanto et al., 2023), while machine learning offers flexible modeling and interpretability via feature importance and SHAP analysis. This combined framework identifies dominant process factors, enhances optimization reliability, and advances data-driven microplastic removal strategies for sustainable water treatment.

METHOD

Materials

Iron(II) sulfate heptahydrate ($FeSO_4 \cdot 7H_2O$), PAM, sodium bicarbonate ($NaHCO_3$), sodium hydroxide (NaOH), and hydrochloric acid (HCl) were procured from Sigma Aldrich Chemical, USA. Deionized (DI) water was procured from Hanna Hi, Indonesia. Commercially available PET, PE, and PP plastics were acquired from EntertainmentFG and Aneka PVC Curtain, Indonesia. Microplastic particles were prepared using a two-step mechanical process. Bulk PET material was first abraded with an iron file to generate coarse fragments, which were then ground with a mortar and pestle under ambient conditions. The resulting particles were subsequently sieved using wire meshes into three size fractions based on diameter: d_1 < mesh 1, mesh 1 < d_2 < mesh 2, and mesh 2 < d_3. The diameters of the wire-meshes were (48.1 ± 3.3) µm and (99.2 ± 6.7) µm for mesh 1 and mesh 2, respectively. Prior to the grinding process, the plastics were cleansed with 0.1 M HCl solution to eliminate impurities. This process is illustrated in **Figure S1a**.

Coagulation Process and Microplastics Removal Efficiency

Coagulation experiments were conducted in 0.5 L beakers with stirring. A 0.1 M $NaHCO_3$

buffer solution was prepared in DI water, with pH adjusted using 0.1 M HCl or NaOH. Then, 0.1 g microplastics (200 mg/L initial concentration) were added, followed by $FeSO_4 \cdot 7H_2O$ coagulant and PAM coagulant aid. Solutions were mixed at 300 rpm for 1 min, then 100 rpm for 14 min, and rested for 30 min for sedimentation (**Figure S1b**). The elevated concentration was chosen for reliable gravimetric quantification across polymers and sizes. For Box–Behnken design (BBD), 15 runs per polymer (PE, PP, PET) across three size classes yielded 135 experiments, with single runs per condition but triplicates at RSM-optimized conditions for validation (mean ± standard deviation).

Removal efficiency was determined by comparing recovered floc mass to initial microplastic mass (Ma et al., 2019a). As shown in **Figure S1c**, flocs were transferred to a Millex™ PVDF syringe ultrafilter (0.1 μm pore, 33 mm, hydrophilic, sterile) to retain microplastics while passing dissolved species. Retained material was washed with 0.1 M HCl to dissolve iron residues without degrading plastics, then filtered under gentle vacuum to minimize particle loss. Samples were dried in a vacuum desiccator (Normax Glass Desiccator Vacuum, Portugal; Rocker Chemker 300 Vacuum Pump, Taiwan) at 25°C for 15 min, a duration confirmed by preliminary trials showing constant mass (**Figure S2**). Dried samples were weighed in duplicate using an analytical balance (HZY-A, Ningbo ETDZ Hansen, China; 0.1 mg resolution). Removal efficiency was then calculated from the recovered dry mass (W_{dried}) and initial mass ($W_{initial}$) per Equation 1,

$$\text{Removal Efficiency MPs} = [(W_{initial} - W_{dried})/ W_{initial}] \times 100\% \quad (1)$$

The morphology of the flocs was investigated using a digital microscope (AmScope MU1000, USA), and the dried flocs were further examined using a scanning electron microscope equipped with Energy Dispersive Spectroscopy (SEM-EDS) (JSM-6510LA, JEOL, USA). The dried microplastics that had been separated from the flocs were also analyzed using Fourier Transform Infrared (FTIR) spectroscopy (IRPrestige-21, Shimadzu, Japan) to confirm the polymer type.

Optimization using RSM and Machine Learning

Optimization employed response surface methodology (RSM) with BBD and machine learning. RSM treated coagulation parameters (**Table 1**) as independent variables and microplastic removal efficiency as the response. Each microplastic type/size class generated 15 randomized BBD runs (12 edge + 3 center points), analyzed via quadratic polynomial models in Minitab 17 (Minitab, LLC, State College, PA, USA) without data transformation. Model adequacy, lack-of-fit, and effects significance ($p < 0.05$) were assessed via ANOVA, with residual diagnostics confirming ANOVA assumptions. Group mean differences were evaluated using ANOVA with Tukey's HSD post hoc test ($\alpha = 0.05$). The resulting dataset informed machine learning optimization for predicting removal efficiency under optimal conditions.

Machine learning used the 15 RSM-generated data points per microplastic type/size class, split consistently into 12 training and 3 testing points across models. Training employed 10-fold cross-validation on training data (1–2 point folds). Hyperparameters were manually tuned based on cross-validation performance. Models included Decision Tree (Tree: binary tree, min

Table 1. Parameters and levels used in the RSM-based coagulation experiments for microplastic removal.

Variable	Level		
	-1	0	1
Coagulant dose (mM/L)	1	3.5	6
PAM dose (mg/L)	0	7.5	15
pH	5	6.5	8

leaf samples = 2, no split < 5 samples, max depth = 200), Random Forest (RF: no split < 5 samples), kNN (5 neighbors, Euclidean distance, uniform weights), SVM (RBF kernel, 100 iterations), Linear Regression (LR: intercept enabled, Ridge L2 regularization), and ANN (100 hidden neurons, ReLU, Adam solver, 1000 max iterations). Model performance was assessed using coefficient of determination (R^2), root mean square error (RMSE), and mean absolute percentage error (MAPE). R^2 measures explained variance (0–1, higher is better) (Qiu et al., 2023), RMSE reflects prediction error in target units (lower is better) (Astray et al., 2023), and MAPE quantifies average percentage prediction error (lower is better) (Fazil et al., 2024). For the best-performing model, SHAP values were computed to quantify each feature's contribution, enabling interpretable and transparent model evaluation (Fazil et al., 2024). All analyses were conducted in Orange Data Mining (Dobesova, 2024).

RESULTS AND DISCUSSION

Microplastics were produced with mean diameters matching wire-mesh sizes: PET (30.48 ± 14.06 µm, 64.40 ± 21.49 µm, 117.49 ± 38.27 µm). PE (35.11 ± 15.17 µm, 71.46 ± 14.19 µm, 121.18 ± 18.56 µm). and PP (28.98 ± 12.34 µm, 79.24 ± 20.34 µm, 129.78 ± 34.05 µm) for d_1 – d_3, respectively. SEM revealed mainly irregular fragments with few pellets and minor fiber-like forms (**Figure 1a**). Size variations in SEM images stem from particle aggregation, overlap, and

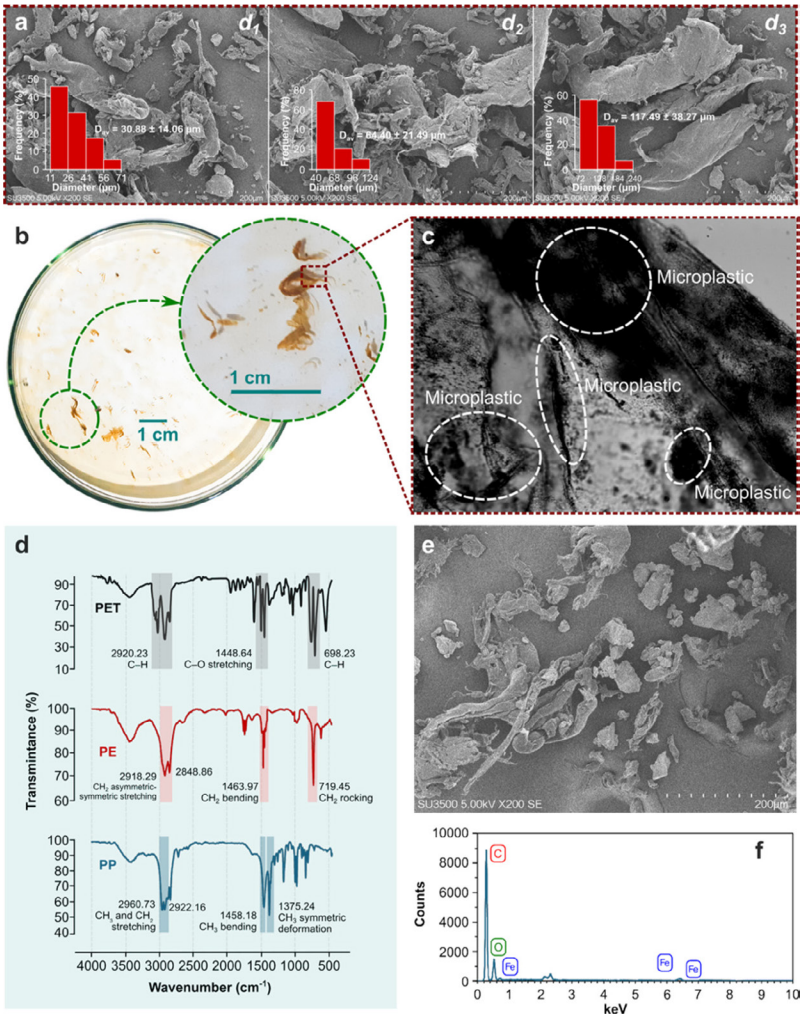

Fig. 1. (a) SEM images of PET microplastics in different size classes (d1–d3); (b) photograph of microplastic flocs in treated water; (c) digital microscope image of floc morphology; (d) FTIR spectra identifying PET, PE, and PP; (e) SEM image of dried flocs; (f) EDS spectra showing floc elements, mainly C, O, and Fe.

Table 2. Removal efficiency of various microplastics from experiment with RSM design.

Run no.	Input level			Response: Removal efficiency (%)								
	Coagulant dose (mM/L)	PAM dose (mg/L)	pH	PET(d_1)	PET(d_2)	PET(d_3)	PE(d_1)	PE(d_2)	PE(d_3)	PP(d_1)	PP(d_2)	PP(d_3)
1	1	7.5	5	17.4	16.9	16.8	19.5	16.7	17	17.1	15.8	18.4
2	1	7.5	8	12.1	12.6	12.5	13.9	10.9	12.3	12.2	11.3	11.9
3	6	7.5	5	80.9	81.4	81.7	82.1	76.7	79.9	80.9	55.6	80.6
4	6	7.5	8	61	62.3	62.7	65.8	60.8	62.5	63	42.4	66.8
5	1	0	6.5	11	10.6	10.8	15.7	10.7	11.2	11	18.7	17.4
6	1	15	6.5	22	20.5	20.7	28.7	19.9	20.9	21.1	33.5	27.8
7	6	0	6.5	60.5	61.5	61.2	65.7	58	61	60.8	23.5	66.9
8	6	15	6.5	87	87.3	87.1	88.7	88	86	86.7	90.7	86.8
9	3.5	0	5	40	39.5	39.8	40.5	41.3	39.7	40.2	19.4	44.7
10	3.5	15	5	68.1	67.9	68.3	68.9	65.9	68.5	68.6	65.8	64.9
11	3.5	0	8	31.4	31.9	31.6	33.9	31.6	32	31.8	19.6	30.7
12	3.5	15	8	64.5	64.2	64	62.7	64.1	64.2	63.7	60.8	55.9
13	3.5	7.5	6.5	52.3	53	52.6	60.3	51.6	52.7	52.1	76.3	52.9
14	3.5	7.5	6.5	51.8	51.8	51.2	58.9	51.9	51.9	51.6	75.5	53.1
15	3.5	7.5	6.5	52	50.9	50.9	59.7	52.4	52	50.7	76.8	53

2D projection effects, but remained consistent with mesh classifications.

Fe-based coagulant with PAM aid effectively removed all microplastic types, entrapping them within dense, aggregated flocs (**Figure 1b–c**), consistent with prior Fe-based studies (Ma, et al., 2019). FTIR confirmed microplastic identity (**Figure 1d**): PET with peaks at ~1710, 1240, and 1100 cm^{-1}; PE at ~2915, 2849, 1472, and 730 cm^{-1}; and PP at ~2950, 2870, 1455, and 1375 cm^{-1}, matching reported spectra (Linares Veliz et al., 2019). SEM–EDS of the dried flocs (**Figure 1e–f**) verified C, O, and Fe composition, confirming successful integration of microplastics within Fe-based coagulated structures. **Table 2** presents the removal efficiencies of three microplastic types under varying coagulant doses, PAM doses, and pH. Results showed that increasing both coagulant and PAM doses significantly improved removal. At the highest tested levels (6 mM/L coagulant, 15 mg/L PAM), efficiencies exceeded 87% for PET, 88% for PE, and 90.7% for PP, confirming the synergistic effect of coagulant–polymer interaction. In contrast, the lowest treatment levels (1 mM/L coagulant, 0 mg/L PAM) yielded only 10–20% removal, indicating weak coagulation. pH also affected performance, with acidic conditions (pH 5) generally yielding higher efficiencies than neutral or alkaline ones. For example, at 3.5 mM/L coagulant, PE and PP removals surpassed 68% at pH 5 but dropped below 60% at pH 8, implying enhanced particle destabilization under acidic environments.

ANOVA results (**Table S1**) confirmed the statistical significance ($p < 0.05$) of all three linear factors, with coagulant dose being the most influential ($p = 0.000$). The quadratic coagulant term was significant for all microplastic types, notably PP(d_2) ($p = 0.000$), suggesting an optimal dosage range before overdosing reduces efficiency. PAM and pH quadratic effects were selectively significant, PAM for PP(d_2) and pH for PE(d_1) and PP(d_2), highlighting conditional sensitivities in coagulation. Predictive RSM equations (**Table S2**) and corresponding R^2 values were derived, identifying optimal removal conditions for each microplastic type, further examined alongside machine learning results in the next section.

RSM contour plots (**Figure 2**) reveal consistent trends across microplastic types and sizes. **Figure 2a** shows PET removal efficiency patterns for all size fractions (d_1–d_3) in coagulant vs PAM dose, coagulant vs pH, and pH vs PAM dose interactions. Coagulant–PAM contours demonstrate that simultaneous increases in both enhance efficiency, while PAM alone yields minimal improvement, emphasizing synergistic balance. Similarly, coagulant dose vs pH plots show pH (5–8) has limited effect without increased coagulant. Optimal removal occurs at pH 5–7, where Fe(III) hydrolyzes into positively charged species $Fe(H_2O)_6^{3+}$, $Fe(OH)^{2+}$, $Fe(OH)_2^{+}$, $Fe_2(OH)_2^{4+}$ that neutralize negatively charged microplastics via charge neutralization. Concurrent

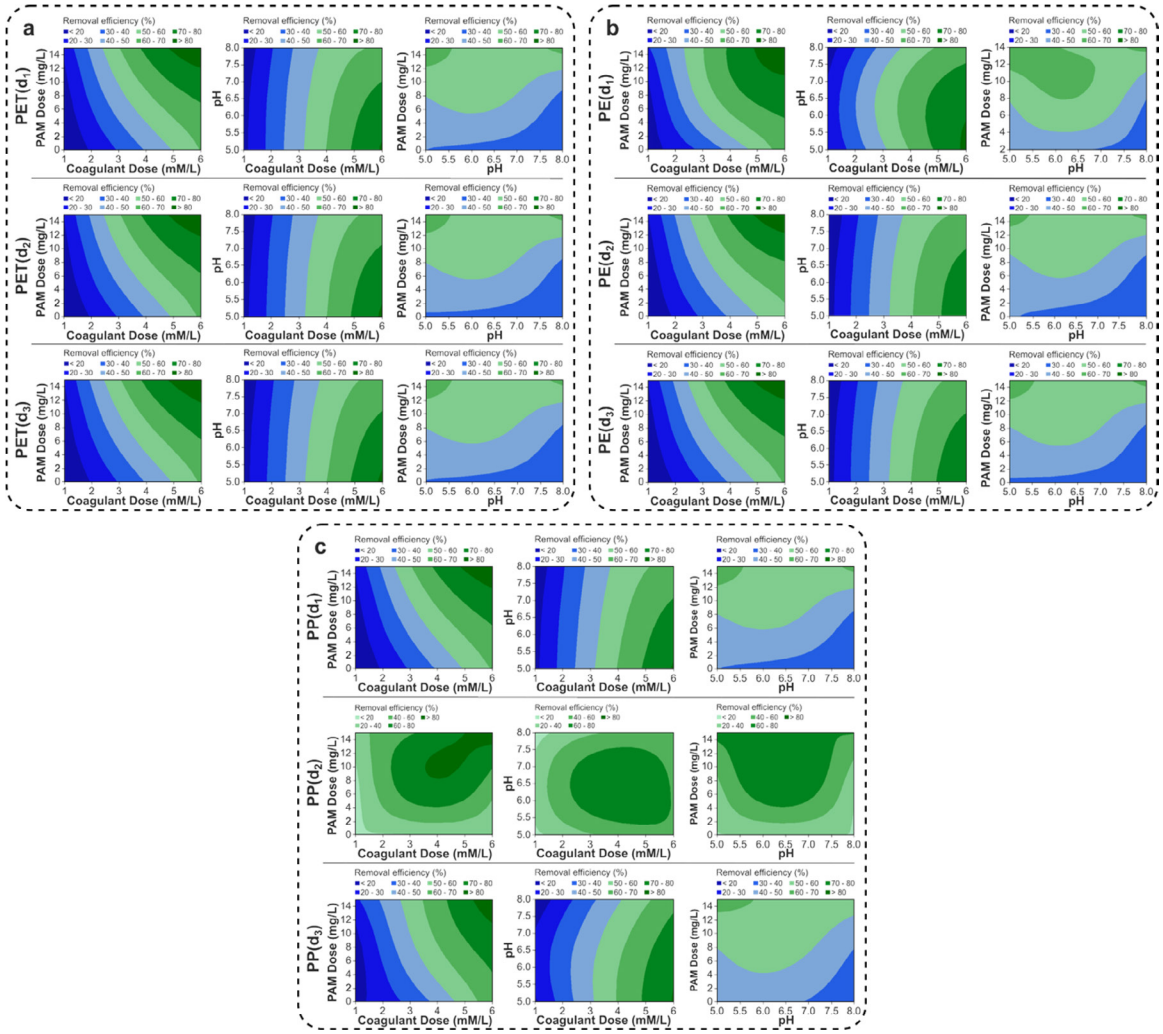

Fig. 2. RSM contour plots showing the effects of coagulation factors on microplastic removal efficiency: (a) PET, (b) PE, and (c) PP.

$Fe(OH)_3(s)$ precipitation at Fe(III) solubility minima (pH 5–7) "sweeps" particles into flocs via enmeshment, avoiding soluble monomers (pH < 5) or polymeric/negative $Fe(OH)_4^-$ (pH > 8). This dual mechanism, optimized by coagulant dose and enhanced by PAM bridging, follows standard iron coagulation chemistry.

This finding aligns with previous research (Rajala et al., 2020), which suggests that acidic to near-neutral pH conditions are conducive to Fe-based coagulation processes. The pH vs PAM dose contours also reflect this trend: at optimal PAM concentrations, removal efficiency significantly improves within a specific pH window. These contour patterns are consistently observed in **Figure 2b** (PE) and **Figure 2c** (PP). Although the PP(d_2) contour in **Figure 2c** may appear slightly distinct at first glance, a closer examination reveals that its overall trend remains consistent with the general pattern observed in other microplastic types, thereby emphasizing the robustness of the factor interactions across microplastics types (Ghernaout et al., 2012; Oriekhova et al., 2014; Ratnayaka et al., 2009).

Machine learning results revealed substantial performance variation across algorithms and microplastic types (**Figure S3**). ANN and LR consistently outperformed other models in RMSE, MAPE, and R^2. On training data, ANN achieved RMSE < 5, MAPE < 0.1, and $R^2 > 0.94$ across all types, for instance PET(d_3): RMSE = 4.283, MAPE = 0.072, $R^2 = 0.972$, closely followed

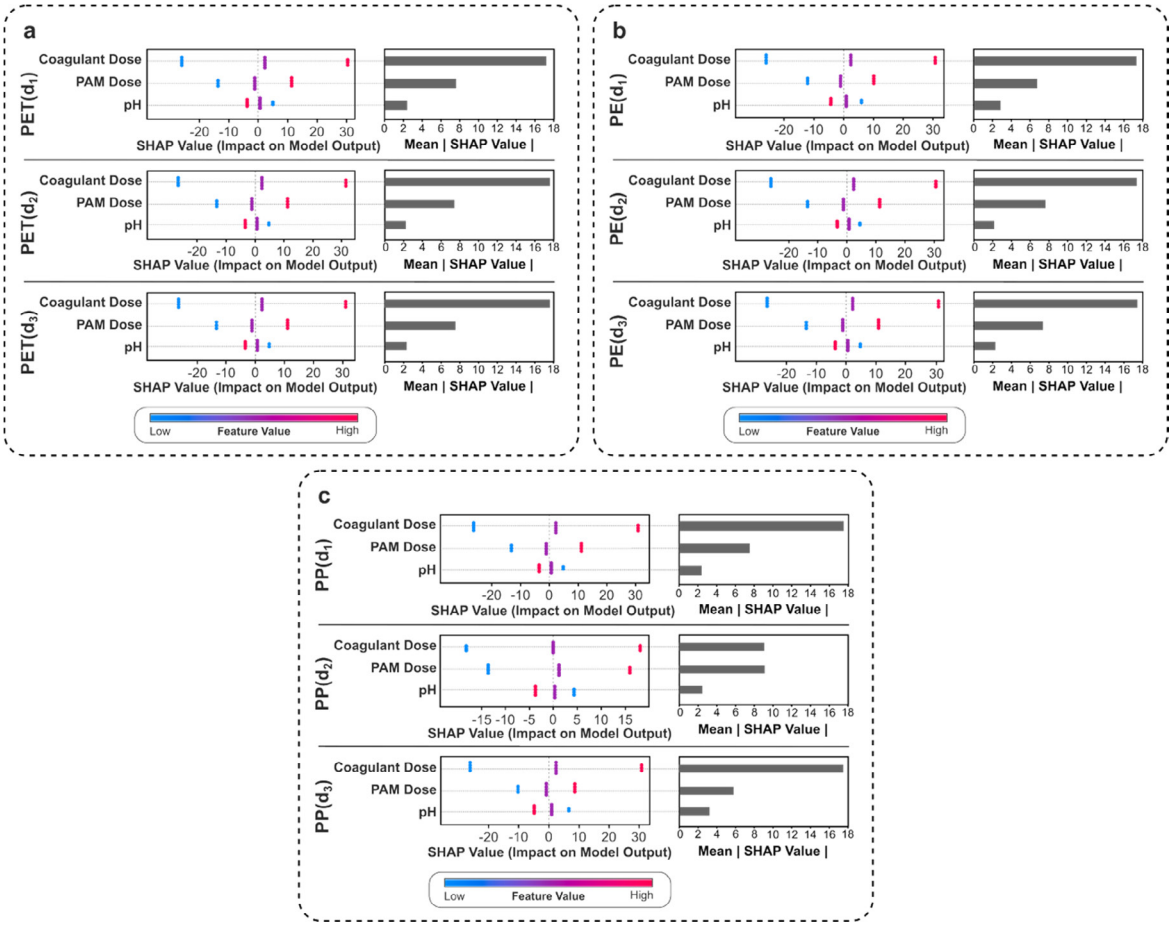

Fig. 3. SHAP value plots from the machine learning model showing the influence of coagulation factors on microplastic removal efficiency: (a) PET, (b) PE, and (c) PP.

by LR. In contrast, kNN and SVM generalized poorly, showing negative R^2 on testing data, for example, PET(d_1) kNN testing: RMSE = 24.21, R^2 = −0.997. Tree and RF showed moderate training R^2 (>0.8) but limited generalization (testing R^2: Tree = −0.1 to 0.25; RF = 0.13 to 0.52), suggesting overfitting. Despite its simplicity, LR demonstrated strong generalizability with high testing R^2 values (e.g., 0.943 for PET(d_1), 0.941 for PET(d_3)), indicating a predominantly linear removal–parameter relationship within the tested range. ANN, though slightly overfitting in some cases, maintained robust testing performance (e.g., PET(d_3): RMSE = 4.287, R^2 = 0.97).

Figures S4–S6 compare predicted vs. actual values and residuals for PET, PE, and PP. RSM yielded consistently high R^2 (0.987–0.993), with residuals randomly scattered around zero, confirming minimal bias. LR and ANN similarly produced strong, consistent R^2 values across all types and sizes in both training and testing, with randomly dispersed residuals indicating reliable, unbiased predictions. SHAP analysis on the best-performing model (LR) revealed a consistent parameter importance ranking across all microplastic types and sizes (**Figure 3**): coagulant dose > PAM dose > pH. Coagulant dose dominated through charge neutralization and sweep flocculation, while PAM synergistically bridged particles to enhance agglomeration. pH influenced functional group ionization and coagulant–microplastic interactions, most effectively under slightly acidic conditions. SHAP dependence plots (**Figure S7**) confirmed that higher coagulant doses drove efficiencies above 80%, PAM showed a similar but weaker trend, and pH was optimal at 5–6, with diminishing returns beyond this range. These machine

Table 3. Removal efficiency of microplastics based on optimum parameters.

Microplastics	Optimum parameters			Removal efficiency (%)						
	Coagulant dose (mM/L)	PAM dose (mg/L)	pH	Experiment	RSM	RSM error	LR	LR error	ANN	ANN error
PET(d_1)	6.00	15.00	5.00	94.9 ± 0.2	95.1	0.23	91.2	4.06	100.0	5.10
PET(d_2)	6.00	15.00	5.00	94.3 ± 0.1	95.7	1.46	91.2	3.40	100.0	5.70
PET(d_3)	6.00	15.00	5.00	93.6 ± 0.3	96.1	2.62	91.3	2.52	100.0	6.40
PE (d_1)	6.00	15.00	5.67	93.3 ± 0.3	93.8	0.56	91.2	2.30	96.0	2.81
PE(d_2)	6.00	15.00	5.00	93.0 ± 0.3	92.2	0.88	90.2	3.10	99.6	6.63
PE(d_3)	6.00	15.00	5.00	92.8 ± 0.4	94.2	1.46	91.0	1.98	99.5	6.73
PP(d_1)	6.00	15.00	5.00	92.3 ± 0.1	95.5	3.38	91.3	1.10	99.8	7.52
PP (d_2)	5.19	15.00	6.30	91.7 ± 0.4	95.4	3.85	87.0	5.40	92.0	0.33
PP (d_3)	6.00	15.00	5.52	90.1 ± 0.5	91.7	1.74	89.4	0.78	93.8	3.94
Average error* (%)						**1.80[a]**		**2.74[b]**		**5.02[c]**

*Significant differences ($p < 0.05$) between groups are indicated by distinct letters, based on Tukey's one-way ANOVA analysis

learning-derived insights closely aligned with RSM contour plots, reinforcing result robustness across methodologies.

RSM optimization identified parameter combinations maximizing microplastic removal across all types and sizes. These optimal conditions were further evaluated using the best-performing ML models, LR and ANN, and compared with experimental results (**Table 3**). Average prediction errors were 1.80% for RSM, 2.74% for LR, and 5.02% for ANN, each statistically distinct. RSM outperformed both ML models, particularly for PET and PP, confirming its robustness under small, structured experimental datasets (Ray et al., 2023). RSM's strength lies in its systematic experimental design, ensuring uniform input coverage and accurate interpolation through interpretable regression models that capture main and interaction effects. In contrast, ML models, especially ANN, typically need large, diverse datasets to generalize effectively. Applied to smaller datasets, they may overfit or learn noise rather than true patterns, reducing predictive reliability (Ying, 2019).

Compared to prior work summarized in **Table 4**, this study demonstrates marked improvements in both removal efficiency and methodological rigor. Earlier studies, such as Wang et al. (2021) and Zhang et al. (2021), reported high removal rates (94% for 3 μm PE; 92.6% for PE ≤ 270 μm) but generally focused on a single polymer and specific coagulant systems without process optimization. In contrast, this study applied Fe-based coagulation across three major polymers (PET, PE, PP) and multiple size ranges. Cross-study comparisons remain challenging due to variations in experimental conditions, such as initial concentrations, water matrices (DI, tap, or wastewater), particle shapes, and coagulant forms. For example, DI or tap water often yields higher efficiencies due to limited organic or colloidal interference, while real wastewater introduces competing substances that hinder charge neutralization. Particle morphology and size also influence performance; spherical microbeads are more easily removed than fragments or fibers, and smaller particles (<10 μm) require stronger coagulation forces. Furthermore, $FeCl_3$ and $FeSO_4$ differ in hydrolysis and floc formation behavior, affecting removal kinetics. Reported efficiencies in **Table 4** should therefore be viewed as system-specific.

Using RSM optimization, this study achieved up to 94.9% removal, substantially higher than Zhang et al. (2020), who reported 13.6% removal for 10–125 μm PE using $Al_2(SO_4)_3$ and

Table 4. Comparison of removal efficiency of microplastics using coagulation methods.

Purification technique	Microplastic type and size	Optimization	Removal efficiency (%)	Reference
Coagulation using $Mg(OH)_2$, Fe_3O_4, and PAM	PE (≤ 270 μm)	Not available	92.6	(Zhang et al., 2021)
Coagulation using $FeCl_3$ and PAM	PE (< 500 μm, 500 – 5000 μm)	Not available	90.9	(Ma et al., 2019a)
Coagulation using polyaluminum chloride (PAC) and $FeCl_3$	PS (< 200 μm, 500 – 1000 μm, and 1000 – 5000 μm)	Not available	77.83	(Zhou et al., 2021)
Coagulation using $Al_2(SO_4)_3$ and polyDADMAC	PE (10 – 20 μm, 45 – 53 μm, and 106 – 125 μm)	Not available	13.6	(Zhang et al., 2020)
Coagulation using $Al_2(SO_4)_3$ and polyamine-coated sand	PE (10 – 100 μm)	Not available	92.7	(Shahi et al., 2020)
Coagulation using PAC, $FeCl_3$, polyferric sulfate (PFS), Alum, $Al_2(SO_4)_3$, and $FeSO_4$	PE (3 μm)	Not available	94	(Wang et al., 2021)
Coagulation using $AlCl_3$, $FeCl_3$ and PAM	PE (< 500 μm, 500 – 5000 μm)	Not available	61.19	(Ma et al., 2019b)
Coagulation using $Fe_2(SO_4)_3$ and $Al_2(SO_4)_3$	PVC (< 50 μm)	Optimization of reaction conditions	≈ 80	(Prokopova et al., 2021)
Flocculation using $MgCl_2$ and $AlCl_3$	PS (0.05 – 0.1 μm)	Not available	> 90	(Chen et al., 2021)
Coagulation using $AlCl_3$ and $CaCl_2$	PS (0.1 μm)	Not available	> 80	(Chen et al., 2020)
Coagulation using $FeSO_4$ and PAM	PET, PE, and PP (< 48.1 μm, 48.1 – 99.2 μm, and > 99.2 μm)	RSM and machine learning	90.1 – 94.9	**This work**

polyDADMAC. The integrated RSM–machine learning framework enabled precise prediction and revealed nonlinear factor interactions often overlooked previously. While earlier works (Ma et al., 2019b; Chen et al., 2021) examined various coagulant types, they lacked integrated optimization and interpretability. Thus, this study not only demonstrated superior efficiency but also introduced a scalable, data-driven approach that deepens understanding of coagulation dynamics and informs future water treatment strategies.

Limitations and Future Prospects

Several limitations should be considered when interpreting these findings. First, RSM (BBD) design used single experimental runs per microplastic type and size, with replication only at optimized conditions. This limited statistical robustness and prevented full quantification of variability. Future work should include replicates across the full design space to improve reliability and uncertainty estimation. Second, the machine learning dataset comprised only 15 points per polymer–size combination, restricting model complexity. Under such small, structured datasets, simpler models like linear regression outperform complex algorithms such as ANN, which require larger, more diverse data. Hence, the ML results here should be viewed as exploratory. Expanding datasets with varied matrices, microplastic types, and parameters will enable more robust model development. Third, residual dissolved Fe concentrations were not measured, though they are relevant for water quality and compliance. Elevated Fe may affect aesthetics or downstream processes, highlighting the need for future studies to measure residuals and evaluate post-treatment options such as filtration or adsorption. Additionally, the initial microplastic concentration (200 mg/L) exceeded typical environmental levels (μg/L–mg/L). Although chosen for method development and consistent quantification, future research should test lower, environmentally relevant levels and complex matrices to assess scalability. Lastly, this work focused on removal efficiency and excluded operational aspects like floc

kinetics, sludge generation, and sludge fate. Future research should address these factors to ensure the sustainability and safety of Fe-based coagulation in real-scale water treatment.

CONCLUSIONS

This study demonstrated that iron-based coagulation is highly effective for microplastic removal, achieving up to (94.9 ± 0.2)% efficiency across PET, PE, and PP of various sizes. Integrating RSM with machine learning enabled process optimization, with RSM yielding the lowest mean prediction error (1.80%) compared to LR (2.74%) and ANN (5.02%). Although RSM outperformed ML under small, structured datasets, ML methods are expected to excel with larger, more diverse data. RSM remains ideal for systematically designed experiments that capture factor interactions and nonlinear patterns. Coagulant dose was the most influential factor, followed by PAM dose and pH. Optimal operating conditions were an Fe coagulant dose of ~5–6 mM/L, PAM dose of a few mg/L, and pH 5–7, balancing performance and practicality. These dosages align with typical water treatment practices, underscoring cost feasibility and scalability. RSM and ML serve complementary roles, RSM for mechanistic, design-based optimization and ML for complex, data-rich scenarios. Their integration provides a powerful, predictive framework for advancing microplastic removal and supporting sustainable water treatment strategies.

ACKNOWLEDGEMENTS

Aan Priyanto gratefully acknowledges the Indonesian Endowment Fund for Education (LPDP) for providing master-doctoral scholarships and supporting this research.

GRANT SUPPORT DETAILS

This research is funded by the Indonesian Endowment Fund for Education (LPDP) on behalf of the Indonesian Ministry of Higher Education, Science and Technology and managed under the EQUITY Program (Contract No. 4298/B3/DT.03.08/2025).

CONFLICT OF INTEREST

The authors declare that there is not any conflict of interests regarding the publication of this manuscript. In addition, the ethical issues, including plagiarism, informed consent, misconduct, data fabrication and/ or falsification, double publication and/or submission, and redundancy has been completely observed by the authors.

LIFE SCIENCE REPORTING

No life science threat was practiced in this research.

REFERENCES

Astray, G., Soria-Lopez, A., Barreiro, E., Mejuto, J. C., & Cid-Samamed, A. (2023). Machine Learning to Predict the Adsorption Capacity of Microplastics. Nanomater., *13*(6).

Bahrani, F., Mohammadi, A., Dobaradaran, S., De-la-Torre, G. E., Arfaeinia, H., Ramavandi, B., Saeedi, R., & Tekle-Röttering, A. (2024). Occurrence of microplastics in edible tissues of livestock (cow and sheep). Environ. Sci. and Pollut. Res., 31(14), 22145–22157.

Bhavsar, P. S., Solanki, M. B., Shimada, Y., Kamble, S. B., Patole, S. P., Kolekar, G. B., & Gore, A. H.

(2024). Microplastic contamination in Indian rice: A comprehensive characterization and health risk assessment. J. Hazard. Mater., 480, 136208.
Bratby, J. (2016). Coagulation and Flocculation in Water and Wastewater Treatment (3rd ed.). IWA Publishing, London.
Chartres, N., Cooper, C. B., Bland, G., Pelch, K. E., Gandhi, S. A., BakenRa, A., & Woodruff, T. J. (2024). Effects of Microplastic Exposure on Human Digestive, Reproductive, and Respiratory Health: A Rapid Systematic Review. Environ. Sci. Technol. 2024, 58, 52, 22843–22864.
Chen, Z., Huang, Z., Liu, J., Wu, E., Zheng, Q., & Cui, L. (2021). Phase transition of Mg/Al-flocs to Mg/Al-layered double hydroxides during flocculation and polystyrene nanoplastics removal. J. Hazard. Mater., 406, 124697.
Chen, Z., Liu, J., Chen, C., & Huang, Z. (2020). Sedimentation of nanoplastics from water with Ca/Al dual flocculants: Characterization, interface reaction, effects of pH and ion ratios. Chemosphere, 252, 126450.
Dobesova, Z. (2024). Evaluation of Orange data mining software and examples for lecturing machine learning tasks in geoinformatics. Comput. Appl. Eng. Educ. 32(4), e22735.
Fazil, A. Z., Gomes, P. I. A., & Sandamal, R. M. K. (2024). Applicability of machine learning techniques to analyze Microplastic transportation in open channels with different hydro-environmental factors. Environ. Pollut., 357, 124389.
Garfansa, M. P., Zalizar, L., Husen, S., Triwanto, J., Ramadani, S. D., Iswahyudi, I., & Ekalaturrahmah, Y. A. C. (2024). Research and Trends of Filtration for Removing Microplastics in Freshwater Environments. Environ. Qual. Manag., 34(1).
Ghernaout, D., & Ghernaout, B. (2012). Sweep flocculation as a second form of charge neutralisation—a review. Desalination and Water Treatment, 44(1-3), 15-28.
Huo, Z., Liu, Y., Yang, R., Dong, G., Lin, X., Yang, Y., & Yang, F. (2025). Qualitative and quantitative analysis of microplastics in chicken meat using near-infrared spectroscopy. Microchem. J., 210, 112979.
Linares Veliz, A. B., Jiménez, J. C., López, P., & De Gáscue, B. R. (2019). Biodegradability Study by FTIR and DSC of Polymers Films Based on Polypropylene and Cassava Starch. Orbital: Electro. J. Chem., 11(2).
Liu, X., Shao, J., Peng, C., & Gong, J. (2025). Novel insights related to soil microplastic abundance and vegetable microplastic contamination. J. Hazard. Mater., 484, 136727.
Ma, B., Xue, W., Ding, Y., Hu, C., Liu, H., & Qu, J. (2019a). Removal characteristics of microplastics by Fe-based coagulants during drinking water treatment. J. Environ. Sci., 78, 267–275.
Ma, B., Xue, W., Hu, C., Liu, H., Qu, J., & Li, L. (2019b). Characteristics of microplastic removal via coagulation and ultrafiltration during drinking water treatment. Chem. Eng. J., 359, 159–167.
Mandal, R. (2024). A critical review on microplastics in edible fruits and vegetables: A threat to human health. Multidisciplinary Reviews, 8(3), 2025088.
Oh, H., Sanoev, K., Kim, H., Lee, I., & Hong, T. (2023). *The Removal of Microplastics from Reverse Osmosis Wastewater by Coagulation*.
Oriekhova, O., & Stoll, S. (2014). Investigation of FeCl3 induced coagulation processes using electrophoretic measurement, nanoparticle tracking analysis and dynamic light scattering: Importance of pH and colloid surface charge. Colloids and Surfaces A: Physicochemical and Engineering Aspects, 461, 212-219.
Priyanto, A., Rohman, Y. M., Hapidin, D. A., Edikresnha, D., & Khairurrijal, K. (2023). Rotary Forcespun Polyvinylpyrrolidone Fibers Matrix Loaded with Virgin Coconut Oil: Physicochemical Characterization, In Vitro Antioxidant Assessment, and Release Profile. Food and Bioprocess Technology, 17, 1926-1941.
Prokopova, M., Novotna, K., Pivokonska, L., Cermakova, L., Cajthaml, T., & Pivokonsky, M. (2021). Coagulation of polyvinyl chloride microplastics by ferric and aluminium sulphate: Optimisation of reaction conditions and removal mechanisms. J. Environ. Chem. Eng., 9(6), 106465.
Qiu, Y., Li, Z., Zhang, T., & Zhang, P. (2023). Predicting aqueous sorption of organic pollutants on microplastics with machine learning. Water Res., 244, 120503.
Rajala, K., Grönfors, O., Hesampour, M., & Mikola, A. (2020). Removal of microplastics from secondary wastewater treatment plant effluent by coagulation/flocculation with iron, aluminum and polyamine-based chemicals. Water Res., 183, 116045.
Ratnayaka, D. D., Brandt, M. J., Johnson, K. M. (2009). CHAPTER 7 - Storage, Clarification and

Chemical Treatment. Water Supply (Sixth Edition), 267-314.
Ray, S., Haque, M., Ahmed, T., & Nahin, T. T. (2023). Comparison of artificial neural network (ANN) and response surface methodology (RSM) in predicting the compressive and splitting tensile strength of concrete prepared with glass waste and tin (Sn) can fiber. J. King Saud Univ. Eng. Sci., 35(3), 185–199.
Rossatto, A., Arlindo, M. Z., Morais, M. S., de Souza, T. D., & Ogrodowski, C. S. (2023). Microplastics in aquatic systems: A review of occurrence, monitoring and potential environmental risks. Environ. Adv., 13, 100396.
Shahi, N. K., Maeng, M., Kim, D., & Dockko, S. (2020). Removal behavior of microplastics using alum coagulant and its enhancement using polyamine-coated sand. Process Saf. Environ. Prot., 141, 9–17.
Shen, M., Zhang, Y., Almatrafi, E., Hu, T., Zhou, C., Song, B., Zeng, Z., & Zeng, G. (2022). Efficient removal of microplastics from wastewater by an electrocoagulation process. Chem. Eng. J., *428*, 131161.
Tan, J., Huang, Y., Chi, B., Xiong, Z., Zhou, W., Yang, Z., Zhou, K., Ruan, X., Duan, X., Wang, M., & Zhang, J. (2024). Comparative study of iron and aluminium coagulants in conditioning sludge: Sludge dewatering performance, physicochemical properties, and risk of heavy metal migration. J. Environ. Chem. Eng., 12(4), 113168.
Tang, W., Li, H., Fei, L., Wei, B., Zhou, T., & Zhang, H. (2022). The removal of microplastics from water by coagulation: A comprehensive review. Scie. Total Environ., 851, 158224.
Thathsarani, N., Khiadani, M., Azhar, M. R., & Zargar, M. (2025). Enhanced removal of microplastic fibres using aluminium and chitosan-based coagulants assisted with microbubble technology. J. Environ. Chem. Eng., 13(3), 116780.
Tursi, A., Baratta, M., Easton, T., Chatzisymeon, E., Chidichimo, F., De Biase, M., & De Filpo, G. (2022). Microplastics in aquatic systems, a comprehensive review: origination, accumulation, impact, and removal technologies. RSC Adv. 12(44), 28318-28340.
Wang, X.-S., Song, H., Liu, Y.-L., Pan, X.-R., Zhang, H.-C., Gao, Z., Kong, D.-Z., Wang, R., Wang, L., & Ma, J. (2021). Quantitively Analyzing the Variation of Micrometer-Sized Microplastic during Water Treatment with the Flow Cytometry-Fluorescent Beads Method. ACS ES&T Eng., 1(12), 1668–1677.
Yin, J., Zhu, T., Li, X., Wang, F., & Xu, G. (2025). Phytoremediation of microplastics by water hyacinth. Environ. Sci. Ecotechnology, 24, 100540.
Ying, X. (2019). An Overview of Overfitting and its Solutions. J. Phys. Conf. Ser., 1168, 022022.
Zhang, Y., Diehl, A., Lewandowski, A., Gopalakrishnan, K., & Baker, T. (2020). Removal efficiency of micro- and nanoplastics (180 nm–125 μm) during drinking water treatment. Sci. Total Environ., 720, 137383.
Zhang, Y., Zhao, J., Liu, Z., Tian, S., Lu, J., Mu, R., & Yuan, H. (2021). Coagulation removal of microplastics from wastewater by magnetic magnesium hydroxide and PAM. Journal of Water Process Engineering, 43, 102250.
Zhou, G., Wang, Q., Li, J., Li, Q., Xu, H., Ye, Q., Wang, Y., Shu, S., & Zhang, J. (2021). Removal of polystyrene and polyethylene microplastics using PAC and FeCl3 coagulation: Performance and mechanism. Sci. Total Environ., 752, 141837.
Ziembowicz, S., & Kida, M. (2024). The effect of water ozonation in the presence of microplastics on water quality and microplastics degradation. Sci. Total Environ., 929, 172595.